Atomic and electronic structure of Li-adsorbed Si(100) surfaces

Young-Jo Ko and K. J. Chang
Department of Physics, Korea Advanced Institute of Science and Technology, Taejon 305-701, Korea

Jae-Yel Yi
Department of Physics, Dong-A University, Pusan 602-714, Korea
(Received 30 April 1997)

We investigate the atomic and electronic structure of Li-adsorbed Si(100) surfaces through first-principles pseudopotential calculations. We find that Li adatoms interact mainly with the dangling-bond orbitals of Si dimers, however, no hydrogenlike directional bonds exist between the Li and substrate Si atoms, based on calculated scanning tunneling microscopy images. The analysis of charge densities demonstrates a large charge transfer from the Li adatom to a dangling-bond orbital of a Si dimer, which is responsible for a large decrease of work function at submonolayer coverages. The Li atoms form linear chains either by occupying the interdimer bridge sites along the dimer row direction or the dimer bridge and cave sites perpendicular to the dimer row. As Li coverage (Θ) increases, repulsive interactions between the adatoms in the chains are also found to increase. Thus, at 1-ML Li coverage, the stable adsorptions sites are changed to either the cave and pedestal sites or the valley-bridge and pedestal sites, with all the Si dimers symmetric, resulting in a 2×1 structure. From the calculated formation energies, we find a 1×1 phase to be thermodynamically stable at $\Theta=2$, in contrast to other alkali-metal adsorptions. [S0163-1829(97)09739-7]

I. INTRODUCTION

Alkali-metal adsorption on Si(100) surfaces has been studied intensively over the last decades because of its technological and scientific interests.[1] Although in early days Levine proposed that alkali-metal atoms on the Si(100) surface reside on the pedestal sites (see Fig. 1),[2] there is still some controversy as to the adsorption sites, the bonding character between alkali-metal and substrate Si atoms, and the saturation coverage.[3–10] Later, a double-layer model, where alkali-metal atoms occupy the pedestal and valley-bridge sites at the saturation coverage, was suggested for both Na- and K-adsorbed Si(100) systems,[3] and this model was supported by several first-principles pseudopotential calculations.[11–13] On the other hand, Mangat *et al.* reported a different single site model for the Na/Si(100) system,[14] in which alkali-metal atoms occupy the cave sites.

The structural models for Li-adsorption are quite different from those for other alkali metals. For Na, K, and Cs adsorptions, the 2×1 reconstruction of a clean Si(100) surface was shown to be recovered at the saturation coverage,[6–9,14] while an 1×1 low energy electron diffraction (LEED) pattern was found for Li-adsorbed Si(100) surfaces.[8] Some experiments exhibited Li-induced 2×2 phases at submonolayer coverages with a complex series of the LEED patterns before the 1×1 phase is developed.[15,16] A scanning tunneling microscopy (STM) study with a small amount of Li atoms on the Si(100) surface showed a bright spot on top of the Si dimer row, and suggested that Li adatoms reside on top of the Si dimer atoms, forming hydrogenlike covalent bonds and stabilizing asymmetric dimerization.[5] In core-level spectroscopy measurements, only one core level associated with the Li 1*s* state was observed up to 1-ML coverage, suggesting weak Li-Li interactions and Li adsorption at equivalent sites.[15] Based on STM and core-level spectroscopy studies, the adsorption geometry at 1-ML coverage was proposed to resemble the monohydride structure.[15] However, previous pseudopotential calculations at 1-ML coverage reported two high-symmetry adsorption sites, which are inequivalent, similar to other alkali metals.[17] At present, no clear explanation about this discrepancy has been given, and a complete picture for the adsorption site and the bonding nature at different adsorption coverages is needed.

In this work we perform first-principles pseudopotential calculations for the equilibrium structures and electronic properties of Li-adsorbed Si(100) surfaces at various coverages, with the $p(2\times2)$ structure chosen as a Si(100) substrate. From the calculated STM images for a single Li adatom, we find that the Li adatoms donate their electrons to the dangling bond orbitals of the substrate Si dimers, similar to other alkali metals, while, at low Li coverages, Li atoms favor lower symmetry sites such as the interdimer bridge sites. The charge transfer from the Li adatoms to the Si dimers results in the symmetrization of the substrate Si dimers, and induces large decreases in the work function at submonolayer coverages. As the Li coverage increases to

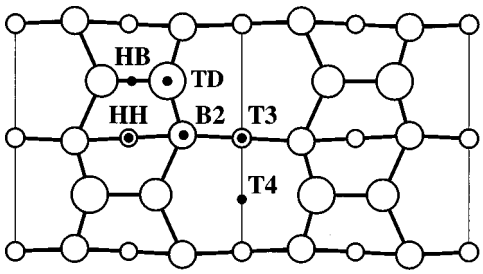

FIG. 1. A top view of the Si(100)$-p(2\times2)$ structure. The pedestal, valley bridge, cave, interdimer bridge, dimer bridge, and hydrogen adsorption sites are denoted by HH, *T*3, *T*4, *B*2, HB, and TD, respectively.

1-ML, repulsive interactions increase between the linear chains formed by the Li atoms at the interdimer-bridge sites, and the surface states that are originated from the Si dangling bonds are completely filled by the Li electrons, which tend to occupy more high-symmetry sites. The thermodynamic stability of various Li-induced surface phases is discussed by comparing their formation energies, and the calculated work functions are compared with experiments at different Li coverages.

II. CALCULATIONAL METHOD

The total-energy calculations are performed using a first-principles pseudopotential method within the local-density-functional approximation.[18,19] Norm-conserving soft pseudopotentials are generated by the scheme of Troullier and Martins,[20] and transformed into the separable form of Kleinman and Bylander.[21] The Wigner interpolation formula is used for the exchange and correlation potential.[22] The partial core correction scheme proposed by Louie, Freyen, and Cohen[23] is employed for the Li potential. The lattice constant of bulk Li in a body-centered-cubic structure is calculated to be 3.403 Å with the core correction, as compared to the measured value of 3.491 Å. The wave functions are expanded in a plane-wave basis set with a kinetic-energy cutoff of 10 Ry and eight **k** points in the irreducible sector of the 2×2 surface Brillouin zone are used for the Brillouin-zone summation of the charge density. Surfaces are modeled by a repeated slab geometry consisting of ten Si layers and a vacuum region with a thickness of eight Si layers inserted between the Si slabs. The Li adatoms are adsorbed on both the surfaces of the Si slab. To obtain the equilibrium configuration, all the ions except for two Si layers centered in the bulk region are relaxed via the conjugate gradient method until the magnitudes of the Hellmann-Feynman forces[24] are less than 3.0 m Ry/a_B, where a_B is the Bohr radius. For band-structure calculations, we employ six-layer slab geometry with one surface passivated by hydrogen.

III. RESULTS AND DISCUSSION

As a starting configuration of the Si(100) substrate, we choose the $p(2\times2)$ structure where dimers are buckled alternatively along the dimer row direction, as shown in Fig. 1. The surface energy of the clean $p(2\times2)$ structure was found to be lower by 0.1 eV/dimer than that of the 2×1 asymmetric dimer structure.[13] To find plausible adsorption sites of Li on the $p(2\times2)$ surface, we calculate the adsorption energy ($E_{\rm ad}$) per Li atom, which is defined as

$$E_{\rm ad}=-(E_{\rm Si+Li}-E_{\rm Si}-nE^{a}_{\rm Li})/n, \qquad (1)$$

where $E_{\rm Si}$ and $E_{\rm Si+Li}$ are the total energies of the clean and Li-adsorbed Si(100) surfaces, respectively. $E^{a}_{\rm Li}$ is the total energy of a spin-polarized free Li atom, and n denotes the number of Li atoms adsorbed on the surface. The calculated adsorption energies and optimized geometries at 1/4-, 1/2-, 1-, and 2-ML Li coverages ($\Theta=\frac{1}{4}$, $\frac{1}{2}$, 1, and 2) are listed in Tables I and II, respectively, for various adsorption sites.

TABLE I. Calculated adsorption energies ($E_{\rm ad}$ in eV) for various adsorption sites (see Fig. 1) at $\Theta=\frac{1}{4}$, $\frac{1}{2}$, 1, and 2 are compared.

Θ	Adsorption sites	$E_{\rm ad}$ 2×2	2×1	1×1
$\frac{1}{4}$	$B2$	2.48		
	HH	2.42		
	$T4$	2.35		
	$T3$	2.20		
	TD	1.80		
$\frac{1}{2}$	$B2$-$B2$ (along the dimer row)	2.49		
	$T4$-HB (perpendicular to the dimer row)	2.44		
	$T4$-$T4$		2.33	
	HH-HH	2.29		
	$T3$-$T3$		2.24	
1	$T4$-HH		2.55	
	$T3$-HH		2.54	
	$B2$-$B2$		2.45	
	$T4$-HB		2.35	
2	$T4$-HB (first-deposited layer)			
	$T3$-HH (topmost layer)			2.16
	$T4$-HH (first-deposited layer)			
	$T3$-HB (topmost layer)		2.09	

A. Stable site and STM images for a single Li adatom

Based on STM studies on the Si surface covered by a small amount of Li atoms,[5] the Li atoms were suggested to form hydrogenlike directional bonds with the Si atoms, residing on top of the Si dimer, which is denoted by TD in Fig. 1. This adsorption site is quite different from the results of first-principles calculations.[17] Since all the previous calculations were done at relatively higher coverages, the discrepancy between theory and experiment might be caused by the fact that the adsorption sites depend on Li coverage. Here we first investigate the adsorption site of a single Li adatom, using a supercell with a $c(4\times4)$ lateral periodicity. Although a single H atom favors the TD site, the stable adsorption sites for a single Li atom are found to be the interdimer bridge ($B2$) and cave ($T4$) sites, which have nearly the same energies, while the TD site is highly unfavorable with the energy higher by 0.35 eV/atom.

To search for a possible origin of the discrepancy between the STM study and our pseudopotential calculations, we simulate STM images for the Li adatom on the surface. Figure 2 shows the calculated STM images in a constant-current mode for various adsorption sites, with the bias voltages of ∓1.5 V for the filled- and empty-state images, respectively. When the tip is away from Li, bright spots only appear around the up dimer atoms because of the charge transfer from the down atom to the up atom in the asymmetric dimer. From the filled-state STM images, we find several important features; when the Li atom is located at high-symmetry sites such as $T4$ and $T3$, there are no bright images around the adatom position, disabling the probe of the Li adatom at these positions [see Fig. 2(b)], while, at the $B2$ site, a bright spot is found at a position slightly off the Li-neighboring Si dimer, which is clearly distinguishable from the Si dimer

TABLE II. Calculated Si-Si ($d_{\text{Si-Si}}$) and Li-Si ($d_{\text{Li-Si}}$) bond distances (in units of Å) are given for different geometries at various Li coverages. The amount of buckling of the Si dimer is given in parentheses.

Θ	Adsorption site	$d_{\text{Si-Si}}$	$d_{\text{Li-Si}}$	
0		2.36 (0.65)		
$\frac{1}{4}$	$B2$	2.35 (0.46)	2.51	
	HH	2.36 (0.79)	2.58	2.90
	$T4$	2.34 (0.67), 2.40 (0.36)	2.60	2.70
	$T3$	2.37 (0.61), 2.38 (0.60)	3.10	3.59
$\frac{1}{2}$	$B2$-$B2$	2.38 (0.56), 2.48 (0.18)	2.48	2.55
	$T4$-HB	2.52 (0.00), 2.32 (0.63)	2.47 (HB)	2.62 ($T4$)
	$T4$-$T4$	2.38 (0.00)	2.66	2.66
	$T3$-$T3$	2.45 (0.03)	3.39	3.39
	HH-HH	2.42 (0.35)	2.61	2.70
1	$T4$-HH	2.57 (0.00)	2.66 ($T4$)	2.62 (HH)
	$T3$-HH	2.74 (0.00)	3.17 ($T3$)	2.67 (HH)
	$B2$-$B2$	2.48 (0.00)	2.51	
2	$T4$-HB		2.47 ($T4$, HB)	2.72 ($T4$, HB)
	$T3$-HH		2.80 ($T3$, HH)	2.80 ($T3$, HH)
	$T4$-HH		2.48, 2.70 ($T4$)	2.47, 2.64 (HH)
	$T3$-HB		2.89 ($T3$)	2.53 (HB)

images [see Fig. 2(a)]. Since the size of the Li atom is small and the $T4$ and $T3$ sites are located at nearly the same height as the surface layer, a very small accumulation of charges around the Li adatom makes it difficult to obtain clear images from this atom. On the other hand, the filled-state image at the TD site is found to be similar to experimentally measured one,[5] as shown in Fig. 2(c); however, it should be pointed out that the energy of the TD site is much higher than for the $B2$ site. Thus we expect that the measured STM image is related to the Li atom at the $B2$ site. For H adsorption, the STM image was shown to be very dark around the H atom, and this feature was attributed to the strong covalent bond between the H and Si atoms, which pulls down the dangling-bond state into the bulk band. However, in the case of Li adsorption, we do not see such hydrogenlike directional bonds between the Li and substrate Si atoms. Even if the Li atom occupies the TD site, a relatively brighter spot is located around the Li atom, which indicates a weak bond between the Li and Si atoms. The empty-state image at the $B2$ site is found to be s like, as shown in Fig. 2(d), and the brightest position is located right above the Li adatom, and this feature clearly demonstrates that a charge transfer occurs from the Li adatom to the Si dimers. Thus our results suggest that it is more appropriate to use an empty-state probe for identifying the adsorption position of Li.

In the very low-coverage regime, the adatom geometry of Li may be constrained by the arrangement of the substrate asymmetric Si dimers. Here we test other $c(4\times2)$ structure within a $p(4\times2)$ supercell, which has similar surface energy to that of the $p(2\times2)$ substrate structure. We find that the ionized Li atom at the $T4$ site interacts strongly with two neighboring up Si atoms of the substrate; thus the $T4$ site adsorption is more stable by 0.15 eV than the $B2$ site adsorption. In this case, however, the STM images for both the $T4$ and $B2$ site adsorptions are very similar to those obtained from the $p(2\times2)$ substrate geometry. The filled-state images at the $T4$ site are found to be indistinguishable from those of the Si dimers; thus the $T4$ site adsorption cannot be resolved by the STM images. For the $B2$ site adsorption, both the filled- and empty-states exhibit similar images to those found for the $p(2\times2)$ substrate, with the rearrangement of the asymmetric Si dimer images.

B. $\Theta = \frac{1}{4}$

For $\Theta = 1/4$, one Li atom is adsorbed on the 2×2 surface unit cell, and since adatom-adatom interactions are negligible, the stable adsorption site is mainly determined by interactions between the adatom and substrate Si dimers. Among various adsorption sites considered here, the $B2$ site is found to be most stable, as shown in Table I. The optimized geometry and the charge densities of the filled and empty states, which are derived by summing the eigenstates lying between the Fermi level E_F and $E_F \pm 1.5$ eV, are plotted and compared with those for the clean $p(2\times2)$ structure in Fig. 3. The Li atom at the $B2$ site is located at a distance of 2.51 Å from two neighboring dimer atoms, and 2.85 Å from a second-layer Si atom. The buckling of the two Si dimers within the unit cell is oriented toward the Li adatom, as shown in Fig. 3(c). The substrate Si dimers are asymmetric with a bond length of 2.35 Å, and the height difference between the up and down Si atoms is reduced to 0.46 Å, while the corresponding values were calculated to be 2.36 and 0.65 Å, respectively, on the clean Si(100)$-p(2\times2)$ surface.[13] For other $T3$ and $T4$ positions, their adsorption sites are far from the neighboring Si dimers; thus the bond length and the buckling of the Si dimers are not much changed, as described in Table II.

In Figs. 3(a) and 3(b), the charge densities of the occupied and unoccupied states on the clean $p(2\times2)$ surface, which originate from the two dangling bonds of the Si dimer, are well localized around the up and down Si atoms, respec-

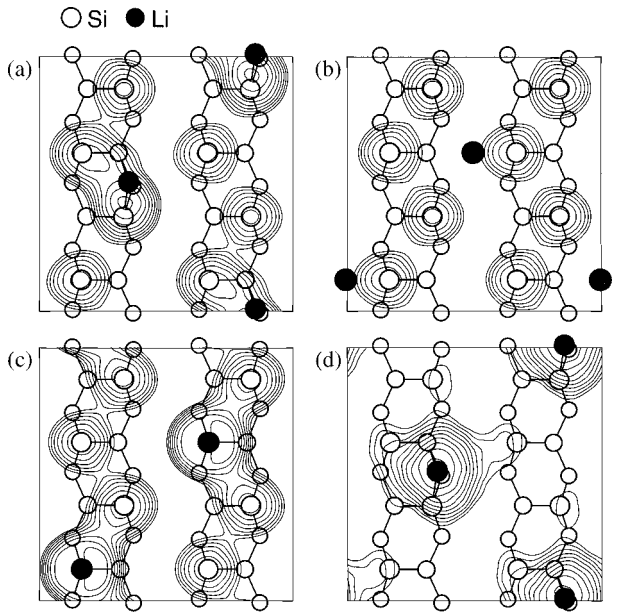

FIG. 2. Calculated constant-current mode STM images are drawn with the bias voltages of ∓ 1.5 V for the filled and empty states, respectively. We show filled-state images for the Li atom adsorbed at (a) the $B2$, (b) $T4$, and (c) TD sites, and (d) an empty-state image for the Li atom at the $B2$ site.

tively. For the $B2$ site adsorption, the occupied state exhibits a pile of charge densities around the up Si atom with some additional accumulation around the down Si atom [see Fig. 3(c)]. Furthermore, the charge densities are well localized above the Si dimer, atoms, and no appreciable charges are found in the Li-Si bonds, as shown in Fig. 3(d). Thus, the main charge transfer occurs from the Li atom to the Si

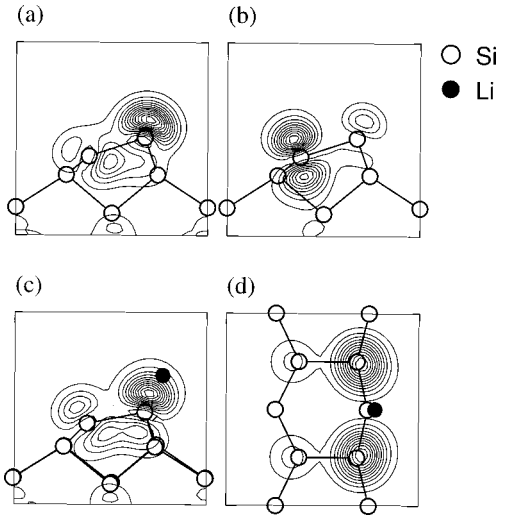

FIG. 3. Optimized geometries and charge density contours, which are obtained by summing the eigenstates lying between E_F and $E_F \pm 1.5$ eV. On the clean $p(2\times2)$ surface, the charge densities of (a) the occupied and (b) unoccupied levels are drawn on a vertical plane containing a Si dimer. For the 2×2 structure with one Li atom at the $B2$ site ($\Theta=\frac{1}{4}$), the charge densities of the occupied surface states are plotted (c) on a vertical plane containing a Si dimer and (d) on a parallel plane lying between the Li atom and its nearest Si atom.

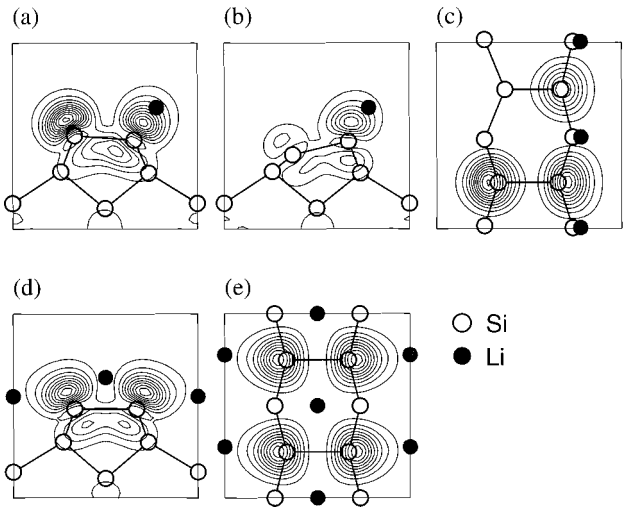

FIG. 4. Optimized geometries and charge densities of the states lying between E_F and $E_F-1.5$ eV for (a)–(c) the 2×2 surface with the two Li atoms at the $B2$ sites ($\Theta=\frac{1}{2}$) and (d) and (e) the 2×1 structure with the two Li adatoms at the $T4$ and HH sites ($\Theta=1$).

dimers, with a partial charge transfer into the down Si atom of the dimer. In this case, because of the more charge accumulation around the up Si atoms, the asymmetric configuration of the dimers is still significant and the buckling is directed toward the Li adatom.

C. $\Theta=\frac{1}{2}$

For $\Theta=\frac{1}{2}$, two Li atoms are adsorbed on the 2×2 surface unit cell. When both the Li atoms occupy $B2$ sites, we choose the optimized geometry of one Li atom adsorbed at the $B2$ site at $\Theta=\frac{1}{4}$ as an initial structure, and then place the other Li atom at one of other equivalent $B2$ sites. In this case, a linear alignment of the Li atoms along the dimer row direction is lower in energy by about 0.2 eV than a zigzag combination of the $B2$ sites or an alignment of Li perpendicular to the dimer rows. This linear geometry is more favorable by 0.05 eV than a linear chain formed by occupying the HB and $T4$ sites perpendicular to the dimer row. In previous calculations, Na and K, which have larger ionic radii, were shown to reside at the $T3$ sites at $\Theta=\frac{1}{2}$.[11–13] In the case of Li, however, the $T3$ sites are found to be least stable among the high-symmetry sites considered here, because of the small size of the Li atom. The energies of the $T4$-$T4$ and $T3$-$T3$ site adsorptions are calculated to be higher by 0.16 and 0.25 eV, respectively, as compared to the stable $B2$-$B2$ site adsorption, and both the geometries show a 2×1 pattern with symmetrized Si dimers.

For the stable $B2$-$B2$ site adsorption, the optimized geometry and the charge densities are plotted in Figs. 4(a)–4(c), and the electronic band structure is drawn in Fig. 5(a). The bond lengths between the Li atoms and their neighboring dimers are estimated to be 2.48 and 2.55 Å, and these values are smaller than for other adsorption sites, as shown in Table II. In this geometry, the two Si dimers within the unit cell have different relaxations; one dimer [see Fig. 4(a)], which has a dimer-bond length of 2.48 Å, is nearly symmetric with a small height difference of 0.18 Å between the dimer atoms, while the other asymmetric dimer [see Fig.

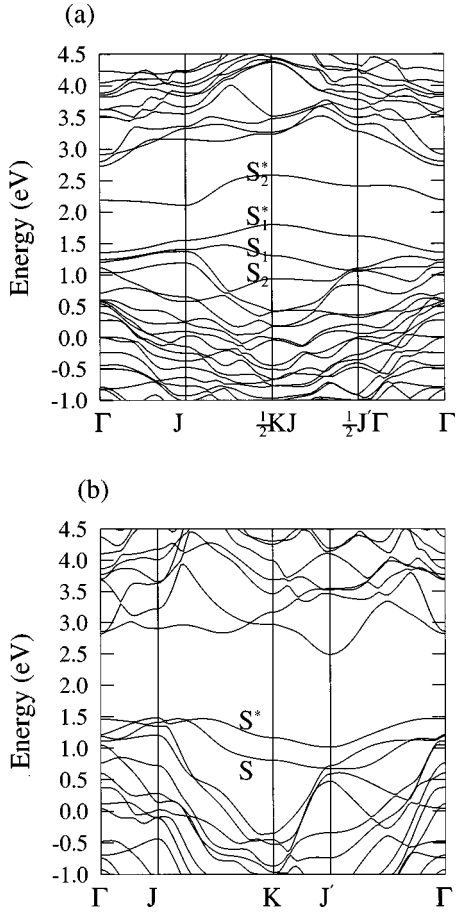

FIG. 5. The electronic band structures along symmetry directions in the surface Brillouin zone for (a) the 2×2 structure with the Li atoms at the $B2$ sites ($\Theta=\frac{1}{2}$), (b) the 2×1 structure with the Li atoms at the $T4$ and HH sites ($\Theta=1$).

4(b)] has a shorter dimer-bond length of 2.38 Å and a height difference of 0.56 Å. Because of the different relaxations, the two dimers exhibit very different charge distributions for the filled state, as shown in Figs. 4(a) and 4(b). The surface band structure in Fig. 5(a) shows that the optimized 2×2 structure is insulating, with a gap energy of 0.31 eV. The surface bands S_1 and S_1^*, which are derived from the nearly symmetric dimer, are fully occupied by two electrons from the Li adatoms, while for the asymmetric dimer only one surface band S_2 originated from the up Si atom is fully occupied.

The linear chain alignment of Li along the dimer row direction is very similar to the 4×1 structure which was found to be the stable geometry of Na-adsorbed Si(100) surface at $\Theta=\frac{1}{4}$.[13] In this case, the ionized Li atoms are surrounded by the negatively charged up atoms of the Si dimers; thus attractive interactions between the Li and Si atoms are more effective. For the $T4$-HB site adsorption, the Li atoms are aligned along the direction perpendicular to the dimer row, with a separation of 7.68 Å between the linear Li chains, and this structure has charge distributions similar to those of the $B2$-$B2$ site adsorption, resulting in similar adsorption energy. When both the Li atoms are located at the $T4$ sites, the bond distance between the Li and Si atoms is 2.66 Å, close to that for the $B2$ sites; however, the adatoms interact less effectively with the Si dangling bond orbitals of p_z shape, because the height of the Li atoms is higher only by 0.2 Å than that of the Si dimers. On the other hand, at the $T3$ sites, the Li-Si bond distance of 3.39 Å is too large for the Li atoms to interact effectively with the dimer atoms. In previous calculations using a 2×1 unit cell,[17] the $B2$ site was reported to be most stable. However, since a 2×1 periodicity is imposed, we find that each dangling-bond orbital is half-filled, and the total energy is increased by 0.14 eV per 2×2 area. The tendency of dangling bond orbitals to be empty or completely filled, so called the negative-U behavior, frequently involves lattice relaxation. In our case, the full occupation of the dangling bond orbital is found to be accompanied by an upward relaxation of the down atom of the sandwiched dimer, leading to the effective electron-electron interaction of $U=-0.14$ eV. Similar negative-U behavior upon alkali-metal adsorption was also reported for a Na-adsorbed GaAs(110) surface.[25]

D. $\Theta=1$

For all the combinations of adsorption sites listed in Table I, the optimized geometries are found to form the 2×1 structure with symmetric dimers. At the coverage of $\Theta=1$, the Li atoms are found to reside on the $T4$ and HH sites rather than on the $B2$ sites. However, the energy difference between the $T4$-HH and $T3$-HH site adsorptions is extremely small, 0.01 eV per 2×1 unit cell. For Li adsorption either at the $T4$-HH or $T3$-HH sites, the Li atoms are well separated from each other, and the dangling-bond orbitals of the Si dimers are fully occupied. When all the Li atoms occupy the $B2$ sites, since repulsive interactions between the neighboring Li chains along the dimer rows are increased, its adsorption energy is reduced, as compared to the cases of $\Theta=\frac{1}{4}$ and $\frac{1}{2}$.

In the optimized geometry of the $T4$-HH site adsorption, the charge densities and the electronic band structure are drawn in Figs. 4(d), 4(e), and 5(b), respectively. In this case, attractive interactions are very effective between the ionized Li atoms and the surrounding charged dimers. The Li-Si bond lengths are calculated to be 2.66 and 2.62 Å for the Li atoms adsorbed at the $T4$ and HH sites, respectively, and the dimer bond is 2.57 Å, while the Li-Si distances for the Li atoms at the $T3$ and HH sites are 3.17 and 2.67 Å, respectively, and the Si dimer is much elongated with a bond length of 2.74 Å. The 1-ML Li-covered surface is found to be insulating because all the surface bands, S and S^* in Fig. 5(b), are completely filled. The two occupied states S and S^* exhibit $pp\pi-$ and $pp\pi^*$-like characters, respectively, and the dimer atoms have a p^3-like bonding configuration, similar to group-V *ad* dimers on Si(100) surfaces. As the Li coverage increases to $\Theta=1$, the surface bands shift to lower energies, similar to other alkali metals,[12] and their splitting is reduced because of the charge transfer from the Li atom to the Si dimer, which induces the symmetrization of the dimers.

E. $\Theta=2$

At $\Theta=2$, the surface structure is quite different from those for other alkali metals. For Na and K adsorptions, the first-monolayer adatoms deposited on the clean Si(100) surface reside on top of the Si layer, and the second deposited

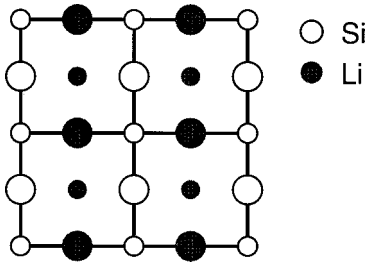

FIG. 6. The optimized geometry for the 1×1 phase at $\Theta=2$.

layer does not interact directly with the Si atoms.[17] Consequently, the substrate keeps a dimerized structure, and the topmost layer over the first deposited alkali metals was shown to be thermodynamically unstable.[13] However, in the case of Li, the first-monolayer Li atoms are positioned deep into the bulk region with nearly the same height as that of the second Si layer of the substrate because of their small atomic size; thus the topmost Li atoms interact directly with the Si dimer atoms. Eventually, all the Si dimer bonds are broken, and a stable 1×1 phase appears. For this coverage, we may speculate a phase shown in Fig. 6, where both the Li and Si atoms are arranged in a 1×1 structure. We find that this phase is more stable by 0.14 eV per 1×1 unit cell than the previously proposed 2×1 structure, in which only the Si atoms are arranged in the 1×1 unit cell, while the Li atoms form a 2×1 structure.[17]

F. Core-level shifts

Here we investigate the surface core-level shift using the final state theory of Pehlke and Scheffler.[32] For the clean $p(2\times2)$ surface, the shifts of the Si $2d$ core levels relative to the bulk atoms are calculated to be -0.49 eV for the up dimer atom, -0.16 eV for the down dimer atom, and 0.05 eV for the second-layer Si atoms, consistent with previous calculations.[26] The observation of a single peak in the Li core-level spectra supports equivalent adsorption sites up to $\Theta=1$.[15] As discussed earlier, our calculations show that the Li atoms reside on two inequivalent adsorption sites at $\Theta=1$, i.e., either the $T4$-HH or $T3$-HH sites. However, we point out that there is a possibility of the $B2$-$B2$ site adsorption, because the $B2$ sites are most favorable at relatively low Li coverages. If the Li atoms reside initially on $B2$ sites at room temperature, which are metastable at $\Theta=1$, thermal annealing of the sample will change the adsorption sites to the $T4$-HH or $T3$-HH sites. For the $T4$-HH site adsorption at $\Theta=1$, the core level of Li at the HH site relative to that at the $T4$ site is calculated to be shifted by 0.14 eV to lower energies.

The core-level shift from the up atom on the clean surface was observed to decrease from -0.50 eV on the clean surface to -0.37 eV for $\Theta=1$, as measured from the bulk peak, doubling its intensity.[15] The change of the core-level shift spectra by Li adsorption can be explained as follows. Additional Li potentials added at the surface would increase the binding energy of the core electrons, while the charge transfer from Li to Si would decrease the binding energy. In addition, the final-state screening effect on the core holes[25] tends to lower the shift to the lower-binding-energy side. Because the up atom already has a full electron occupation on the clean surface, further charge transfer to the up atom does not occur. The screening effect on a core hole in the up atom is not significantly enhanced by Li adsorption because there are no empty states localized on the up atom in the band-gap region.[31] Thus, the position of the core-level shift for the up atom moves to the higher-binding-energy side with increasing Li coverage. The charge transfer from Li to the down atom induces the upward relaxation of the down atom, and the core-level shift of the down atom finally merges with that of the up atom, resulting in the intensity doubling at $\Theta=1$.

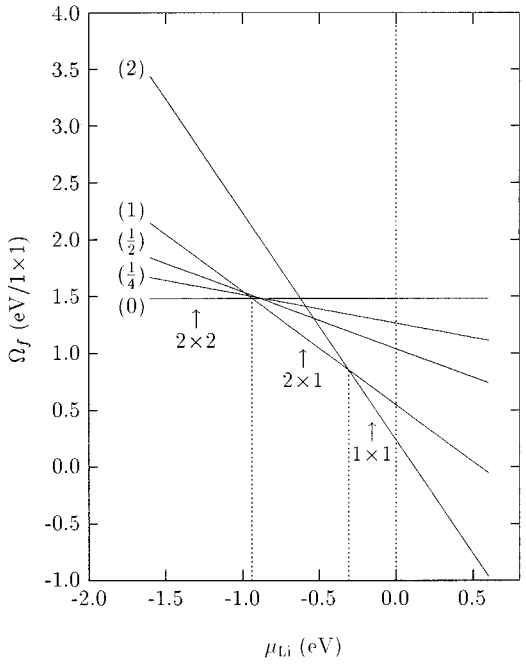

FIG. 7. The formation energies are plotted as a function of the Li chemical potential for each stable structure at coverages $\Theta=\frac{1}{4}$, $\frac{1}{2}$, 1, and 2. The bulk value for μ_{Li} is taken as the origin. The most stable structure is marked by arrows as μ_{Li} increases.

G. Formation energy and stability

The stability of surface structure is examined by calculating the surface formation energy (Ω_f),[27]

$$\Omega_f = E_{\mathrm{Si+Li}} - m\mu_{\mathrm{Si}} - n\mu_{\mathrm{Li}}, \tag{2}$$

where μ_{Si} is the total energy of bulk Si, and n denotes the average number of the Li atoms adsorbed on the 1×1 surface area. In usual experiments, the Li chemical potential (μ_{Li}) is below its bulk value at absolute zero temperature.[28] The calculated formation energies are plotted as a function of μ_{Li} in Fig. 7, with the bulk energy μ_{Li} as the origin. As the Li chemical potential increases, the surface structure changes from the clean Si(100)-$p(2\times2)$ phase to the 2×1 phase of $\Theta=1$, then, to the 1×1 phase of $\Theta=2$. The surface structure maintains the $p(2\times2)$ periodicity of the clean Si surface up to $\mu_{\mathrm{Li}}<-0.94$ eV. As μ_{Li} increases to -0.31 eV, the Li-adsorbed surface exhibits a 2×1 phase at $\Theta=1$. With further deposition of Li, the surface structure becomes a 1×1

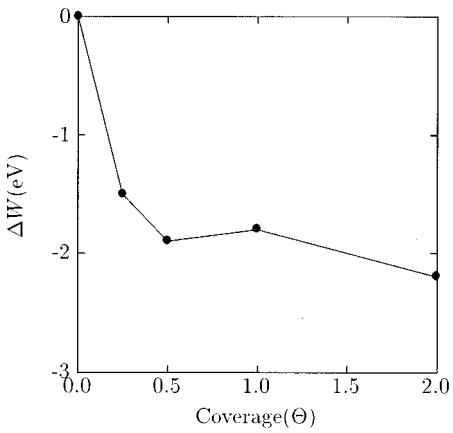

FIG. 8. Work-function change as a function of Li coverage. Filled circles represent our calculated values.

phase at $\Theta=2$. Thus the saturation coverage for the dimerized 2×1 surface corresponds to $\Theta=1$. This structural sequence agrees well with experiments.[8] In previous studies for Na adsorption,[13] the saturation coverage was found to be $\Theta=1$ with a 2×1 phase. For Li adsorption, however, additionally deposited Li atoms over a 1-ML covered surface break the dimers, because of the small size of the Li atom; thus the interactions of Li with the broken dimers reduce the formation energy and stablize the 1×1 structure.

H. Work-function change

The change of work function (ΔW) induced by Li adsorption is calculated and compared with experiments. The work function is defined as the energy difference between the vacuum level and the highest occupied state, which is determined by comparing the valence-band maximum (VBM) level in the bulk region with the occupied surface states. In bulk calculations, we first estimate the position of the VBM relative to the macroscopically averaged electrostatic potential, which is the sum of ionic and Hartree potentials. Then the positions of the highest occupied surface state and the vacuum level are obtained through supercell calculations for surfaces, with respect to the averaged electrostatic potential in the bulklike region. Then, we choose a higher level among the VBM and surface states to compare it with the vacuum level.

The calculated work-function changes are drawn for different Li coverages in Fig. 8. The overall behavior of the work function agrees well with experiments.[8,15,16] Some experiments reported that a Li-induced 2×2 phase appears as ΔW reaches about -1.5 eV.[15,16] Since the formation energy difference between the 2×2 structures found for $\Theta=\frac{1}{4}$ and $\frac{1}{2}$ is very small near $\mu_{\mathrm{Li}}=-0.94$ eV, the observed 2×2 structure may correspond to that of either $\Theta=1/4$ or 1/2. We find that the 2×2 phase with the Li atoms adsorbed at the $B2$ sites at $\Theta=1/4$ has $\Delta W=-1.5$ eV, in good agreement with experiments,[15,16] while the 2×2 structures considered for $\Theta=\frac{1}{2}$ give $\Delta W=-1.9$ and -2.2 eV for the $B2$-$B2$ and $T4$-HB site adsorptions, respectively. The decrease of ΔW at $\Theta=\frac{1}{2}$ mainly results from the depolarized field induced by ionized Li atoms. This depolarization effect becomes more significant, if the Li atoms are adsorbed at the HB, HH, or $B2$ site, the height of which is relatively higher from the surface. At $\Theta=1$, ΔW is estimated to be -1.8 eV, while the value of ΔW at $\Theta=2$ is -2.2 eV for the 1×1 structure, in good agreement with experimental values of -1.8 eV at $\Theta=1$ and -2.35 eV at the saturation coverage.[8,15,16]

The surface dipole moment density (D) satisfies the relation

$$4\pi D=V_{\mathrm{vac}}-V_{\mathrm{bulk}}, \tag{3}$$

where V_{vac} and V_{bulk} represent the average values of the electrostatic potentials in the vacuum and bulk regions, respectively, of the supercell. As Θ increases up to 1, D decreases rapidly due to the Li-induced dipole moments, which have the opposite direction to those on the clean surface. The change of D from the value on the clean surface (ΔD) are calculated to be $-0.22ea_B$, $-0.29ea_B$, and $-0.28ea_B/(1\times1)$ at $\Theta=\frac{1}{4}$, $\frac{1}{2}$, and 1, respectively. The corresponding values per Li adatom are $-0.88ea_B$, $-0.58ea_B$, and $-0.28ea_B$, respectively, indicating that the charge transfer from the Li atoms to the substrate becomes less significant with increasing of Θ. The work function change is affected by both the changes of the dipole layer and the surface band structure by Li adsorption. However, except for the metallic phases at $\Theta=\frac{1}{4}$ and 2, the highest occupied state is associated with the bulk VBM; thus the work-function change is dominated by the change of the dipole layer at the surface. ΔD at $\Theta=2$ is found to be $-0.23ea_B/(1\times1)$ ($-0.12ea_B$ per Li atom), which is larger by $0.05ea_B/(1\times1)$ than that of $\Theta=1$. At $\Theta=2$, however, there is a significant change of the surface structure from those at submonolayer coverages, and the highest occupied state is associated with the broken dimers, which is located much closer to the vacuum level; thus the work function decreases further.

IV. CONCLUSIONS

In conclusion, we have studied the stable geometries of Li-adsorbed Si(100) surfaces through first-principles pseudopotential calculations. Although the Li atoms interact mainly with the dangling-bond orbitals of the substrate dimers, no directional bonds between the Li and Si atoms are found. At $\Theta=\frac{1}{4}$, the interdimer bridge site is found to be most stable, and the analysis of charge densities indicates that the charge transfer occurs from the Li atom to the dangling bonds of the dimers. At $\Theta=\frac{1}{2}$, the Li atoms which occupy the interdimer bridge sites form linear chains along the dimer row direction. In this case, two Si dimers within the 2×2 unit cell show different relaxations; one is nearly symmetric, while the other is asymmetric, resulting in an insulating 2×2 structure. At $\Theta=1$, all the Si dimers are found to be symmetric, and a 2×1 structure is formed with the Li atoms at the pedestal and cave sites, while the substrate dimerization is completely removed at $\Theta=2$.

ACKNOWLEDGMENTS

This work was supported by the MOST, the SPRC at Jeonbuk National University and the CMS at Korea Advanced Institute of Science and Technology.

[1] *Metallization and Metal/Semiconductor Interfaces*, Vol. 195 of *NATO Advanced Study Institute, Series B: Physics*, edited by I. P. Batra (Plenum, New York, 1989).
[2] J. D. Levine, Surf. Sci. **34**, 90 (1973).
[3] T. Abukawa and S. Kono, Phys. Rev. B **37**, 9097 (1988).
[4] H. Tochihara, Surf. Sci. **34**, 90 (1983).
[5] T. Hashizume, I. Sumita, Y. Murata, S. Hyodo, and T. Sakurai, J. Vac. Sci. Technol. B **9**, 742 (1991).
[6] G. S. Glander and M. B. Webb, Surf. Sci. **222**, 64 (1989); **224**, 66 (1989).
[7] C. M. Wei, H. Huang, S. Y. Tong, G. S. Glander, and M. B. Webb, Phys. Rev. B **42**, 11 284 (1990).
[8] L. S. O. Johansson and B. Reihl, Surf. Sci. **287/288**, 524 (1993).
[9] M. Tikhov, G. Boishin, and L. Surnev, Surf. Sci. **241**, 103 (1991).
[10] I. P. Batra, Phys. Rev. B **43**, 12 322 (1991).
[11] B. L. Zhang, C. T. Chan, and K. M. Ho, Phys. Rev. B **44**, 8210 (1991).
[12] K. Kobayashi, Y. Morikawa, K. Terakura, and S. Blügel, Phys. Rev. B **45**, 3469 (1992), and references therein.
[13] Y.-J. Ko, K. J. Chang, and J.-Y. Yi, Phys. Rev. B **51**, 4329 (1995).
[14] P. S. Mangat, P. Soukiassian, K. M. Schirm, L. Spiess, S. P. Tang, A. J. Freeman, Z. Hurych, and B. Delley, Phys. Rev. B **47**, 16 311 (1993).
[15] T. M. Grehk, L. S. O. Johansson, S. M. Gray, M. Johansson, and A. S. Flodström, Phys. Rev. B **52**, 16 593 (1995).
[16] J. W. Chung, C. Y. Kim, K. S. Shin, and K. D. Lee, Surf. Sci. **324**, 8 (1995).
[17] Y. Morikawa, K. Kobayashi, and K. Terakura, Surf. Sci. **283**, 377 (1993).
[18] P. Hohenberg and W. Kohn, Phys. Rev. B **136**, 864 (1964); W. Kohn and L. J. Sham, *ibid.* **140**, A1133 (1965).
[19] C. H. Park, I.-H. Lee, and K. J. Chang, Phys. Rev. B **47**, 15 996 (1993).
[20] N. Troullier and J. L. Martins, Solid State Commun. **74**, 613 (1990); Phys. Rev. B **43**, 1993 (1991); **43**, 8861 (1991).
[21] L. Kleinman and D. M. Bylander, Phys. Rev. Lett. **48**, 1425 (1982).
[22] E. Wigner, Trans. Faraday Soc. **34**, 678 (1938).
[23] S. G. Louie, S. Froyen, and M. L. Cohen, Phys. Rev. B **26**, 1738 (1982).
[24] H. Hellmann, *Einführung in die Quantenchemie* (Deuticke: Leipzig, 1937), p. 285; R. P. Feynman, Phys. Rev. **56**, 340 (1939).
[25] O. Pankratov and M. Scheffler, Phys. Rev. Lett. **71**, 2797 (1993).
[26] E. Pehlke and M. Scheffler, Phys. Rev. Lett. **71**, 2338 (1993).
[27] G. X. Qian, R. M. Martin, and D. J. Chadi, Phys. Rev. B **38**, 7649 (1988).
[28] F. Reif, *Fundamentals of Statistical and Thermal Physics* (McGraw-Hill, New York, 1965).